



## Molecular Crystals and Liquid Crystals

Publication details, including instructions for authors and subscription information:

<http://www.tandfonline.com/loi/gmcl20>

### AFM Studies on Curcumin Based Zn(II) Complex Molecules for Applications as Anticancer Agents

C. M. Tone<sup>a</sup>, S. Pirillo<sup>b</sup>, D. Pucci<sup>b</sup>, M. P. De Santo<sup>a</sup>, R. C. Barberi<sup>a</sup> & F. Ciuchi<sup>a</sup>

<sup>a</sup> IPCF-CNR UOS Cosenza c/o Physics Department, University of Calabria, 87036 Arcavacata di Rende (CS), Italy

<sup>b</sup> Department of Chemistry, University of Calabria, 87036 Arcavacata di Rende (CS), Italy

Version of record first published: 18 Apr 2012.

To cite this article: C. M. Tone, S. Pirillo, D. Pucci, M. P. De Santo, R. C. Barberi & F. Ciuchi (2012): AFM Studies on Curcumin Based Zn(II) Complex Molecules for Applications as Anticancer Agents, *Molecular Crystals and Liquid Crystals*, 558:1, 194-203

To link to this article: <http://dx.doi.org/10.1080/15421406.2011.654188>

PLEASE SCROLL DOWN FOR ARTICLE

Full terms and conditions of use: <http://www.tandfonline.com/page/terms-and-conditions>

This article may be used for research, teaching, and private study purposes. Any substantial or systematic reproduction, redistribution, reselling, loan, sub-licensing, systematic supply, or distribution in any form to anyone is expressly forbidden.

The publisher does not give any warranty express or implied or make any representation that the contents will be complete or accurate or up to date. The accuracy of any instructions, formulae, and drug doses should be independently verified with primary sources. The publisher shall not be liable for any loss, actions, claims, proceedings, demand, or costs or damages whatsoever or howsoever caused arising directly or indirectly in connection with or arising out of the use of this material.

# AFM Studies on Curcumin Based Zn(II) Complex Molecules for Applications as Anticancer Agents

C. M. TONE,<sup>1,\*</sup> S. PIRILLO,<sup>2</sup> D. PUCCI,<sup>2</sup> M. P. DE SANTO,<sup>1</sup>  
R. C. BARBERI,<sup>1</sup> AND F. CIUCHI<sup>1</sup>

<sup>1</sup>IPCF-CNR UOS Cosenza c/o Physics Department, University of Calabria,  
87036 Arcavacata di Rende (CS), Italy

<sup>2</sup>Department of Chemistry, University of Calabria, 87036 Arcavacata di Rende  
(CS), Italy

*We present our recent atomic force microscopy studies on a curcumin based Zn(II) complex anticancer agent. We investigated the morphology of the molecule on a nanoscale level to test the effect of different substrates and solvents on the shape and the aggregation properties of the molecule. Self assembled films were produced by Langmuir technique at different surface pressures and by spin coating.*

*Measurements showed small molecular aggregates with a height of 0,5 nm. The wetting properties of the substrate play a role in the aggregation properties and the film formation. The obtained results will help in understanding the interaction of the studied molecule with DNA or chromonic systems.*

**Keywords** Afm; anticancer molecules; chromonic liquid crystals

## Introduction

The complex studied in this work, [Bpy-9Zn(curc)(Cl)] [1,2], has been selected among the new inorganic complexes recently proposed as effective alternatives to platinum based antitumor agents currently used in chemotherapy [3,4] in order to overcome toxicity and drug-resistance phenomena and to improve activity and selectivity. The synthesis of new metal-based therapeutics is rapidly growing up and these novel complexes show better solubility properties and various substitution kinetics or mechanism pathways, all factors which may induce a pharmacological profile different than those of platinum-drugs. Among them Zinc derivatives are receiving intense interest as promising candidates among the new generation of cytotoxic complexes with low in vivo toxicity and perhaps new modes of action and cellular targets with respect to the classical metallodrugs [5]. Indeed [Bpy-9Zn(curc)(Cl)] shows interesting anti-tumor properties in vitro on several human tumor cell lines, with value of IC<sub>50</sub> of micromolar order [1,2] and high stability in solution, factor that allow it to overcome the curcumin disadvantage of being relatively poor bioavailable and photodegradable. In particular [Bpy-9Zn(curc)(Cl)], is an heteroleptic Zinc(II) complex containing in the same time an N,N chelating ligand (the 2,2'-bipyridine), a diketone

---

\*Address correspondence to C. M. Tone, IPCF-CNR UOS Cosenza c/o Physics Department, University of Calabria, 87036 Arcavacata di Rende (CS), Italy. E-mail: caterina.tone@fis.unical.it

O,O chelating ligand (the curcumin) and a monodentate ligand (chloride), whose overall molecular structure suggests that it may act as metallointercalator.

Moreover, this complex could play also a fundamental role in the chromonic alignment research. We will examine separately the two aspects.

Recently the interest in chromonic liquid crystals is grown and they have found application as low cost linear polarizers, retarders, aligning layer in displays, color filters and in biosensors. Their aggregation properties are under study and trying to align them in homeotropic configuration is a big challenge [6].

Chromonic phases can be considered to be the lyotropic counterpart of discotic phases: the aggregation process is largely driven by enthalpic processes, i.e. the face-to-face attractive forces between chromonogenic molecules [7]. In this category are included dyes, drugs and nucleic acids.

The planar alignment of chromonics has been achieved using Liquid Crystal standard alignments: rubbed polymers, SiO<sub>x</sub>, air or solution fluxes and polymeric gratings; while a metastable homeotropic alignment has been obtained in [8] using DMOAP (N-dimethyl-N-octadecyl-3-aminopropyl trimethoxysilyl chloride).

We believe that a uniform layer of quasi-flat molecules like [Bpy-9Zn(curc)(Cl)] which can interact with aromatic core of chromonic molecules can favour the homeotropic alignment.

A powerful tool for investigating the homogeneity and the mechanical (tribological) properties of the molecular layer is the atomic force microscopy (AFM). It can provide information on the morphology but also on the adhesion of the surfaces.

Several papers show that AFM is also a suitable technique to examine perturbations in the tertiary structure of DNA induced by the binding of a chemotherapeutic agent and, using increment in contour length as a reliable measure of intercalation, revealed saturation occurring at a point where sufficient drug was present to interact with every other available binding site [9–15]. Furthermore is possible to discriminate among different binding mechanism: intercalation, groove binding or covalent attachment [16].

In investigating the DNA-drugs interaction with AFM, the surface can play a fundamental role: the adsorption process can change the DNA conformation and topology and the substrate choice may be critical [17]. For this reason this preliminary study is focused on imaging the anti-tumour molecule on substrates differing for their surface energy and using different solvents in order to verify aggregation phenomena which can compete with the intercalation effectiveness. Two biocompatible solvents (water and ethanol) have been used to prepare samples on solid substrate while, for comparison, samples prepared starting from chloroform solution have been prepared on the same substrates.

## Materials and Methods

[Bpy-9Zn(curc)(Cl)], whose structure is shown in Fig. 1 has been selected because of its long aliphatic chains which makes it suitable for deposition using both Langmuir trough [18] or spin coating.

It has been synthesized as previously described [1,2] through a two steps pathway: in the first step the formation of a Zinc(II) precursor, starting from the bipyridine ligand and the stoichiometric ratio of Zinc chloride, in the second step the reaction between the precursor complex with an equimolar amount of purified curcumin in the presence of triethylamine. [Bpy-9Zn(curc)(Cl)] is soluble in methanol, ethanol, chlorinated solvents and DMSO. The behaviour of Bpy-9Zn(curc)(Cl)] has been investigated by UV/VIS spectroscopy in ethanol

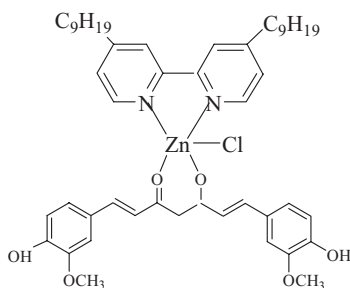


**Figure 1.** Chemical formula of complex [Bpy-9Zn(curc)(Cl)].

solution where it exhibits strong absorption in the UV-vis region, with absorption maximum in the range from 408 to 450 nm. The emission spectrum of [Bpy-9Zn(curc)(Cl)] shows a luminescence maximum at 534 nm with fluorescence yield of 20.4%

[Bpy-9Zn(curc)(Cl)] was deposited on different substrates: silicon wafer was washed in Piranha solution ( $\text{H}_2\text{SO}_4$  and  $\text{H}_2\text{O}_2$ ) in order to remove organic contaminants; glasses were washed in NaOH solutions, sonicated and rinsed several times with Millipore water (18.2 M $\Omega$  cm). Freshly cleaved mica was prepared at the moment of deposition. Hydrophobic glasses, mica and silicon wafer have different surface energy. Mica is widely used in AFM analysis due to its surface smoothness, its transparency, even if it shows birefringence under optical microscopy, and hydrophilicity. On the contrary, carefully cleaned ITO covered glasses are hydrophobic, show a roughness of about 4–5 nm but are suitable for alignment and electric studies of chromonic phases. The analysis has been carried out also depositing layers onto silicon surfaces since they show smoothness like mica but have a different surface energy.

For the deposition of [Bpy-9Zn(CURC)(Cl)] by Langmuir technique, solutions in chloroform at concentration 0.9 mg/mL were prepared. The absence of aggregations phenomena in solution was checked using a quartz cuvette and a spectrophotometer. Films were prepared on Millipore water (18.2 M $\Omega$  cm) using a NIMA 622/D1/D2 film balance with coupled barriers (compression speed 20 cm<sup>2</sup>/min) and transferred via the Langmuir-Blodgett (LB) or Langmuir-Schaefer (LS) techniques onto hydrophilic mica (dipping speed 5 or 10 mm/min), hydrophobic glass substrates and silicon substrates. A micro liter syringe was used to deposit the solution drop by drop onto the water surface. After 10 minutes, necessary for the evaporation of the solvent, the monolayer compression started. Once the pressure deposition was reached, the film was stabilized for 5 min then single layers were transferred into substrates. The transfer ratio was not exactly measurable due to the not regular shape of cut silicon slices but the area versus time graph showed clearly that deposition on the estimated area occurred.

[Bpy-9Zn(curc)(Cl)], was also deposited by spin coating on the same substrates for comparison. It has been performed during the sample rotation for a better coverage at 3000 rpm using a Caltec spin coater. For the deposition of [Bpy-9Zn(curc)(Cl)], by spin coating, solution of [Bpy-9Zn(curc)(Cl)], in chloroform, ethanol and water were prepared at the concentration of 0.9 mg/ml, 1 mg/ml and 10<sup>-4</sup> mg/ml respectively.

A commercial atomic force microscope (NanoScope IIIa, Bruker Inc. Santa Barbara, CA) was used in tapping mode. AFM is a powerful tool to image sample morphology with sub nanometer resolution. In an atomic force microscope a very sharp tip is attached at the end of an elastic cantilever while the sample is moved under the tip using a piezoelectric

scanner. In tapping mode the cantilever oscillates close to its resonant frequency in the free space. When the tip approaches the sample and starts to feel the interaction forces with its surface, the oscillation amplitude changes and the tip hits periodically the sample surface. A built-in AFM feedback circuit works to keep the tip vibration amplitude constant while the scanner movements are used to create the surface morphology image. Silicon cantilevers of the same manufacturer, with a resonance frequency of about 300 KHz were used to acquire the topography of the dried samples in air.

AFM characterization of the deposited films was done after drying for 24 h.

## Results

### Langmuir Deposition

The curve in Fig. 2 reports the surface pressure as a function of area per molecule. When the molecules are far apart they do not interact and the pressure is zero; as soon as they start to interact the pressure raises and the curve slope indicates phase changes at air water interface.

Typical pressure-area curves are reported in Fig. 2. two isotherm cycles were performed just after spreading and 3 hours later. The pressure always starts to raise at about  $85 \text{ \AA}^2/\text{mol}$  and a kink appears in the curve which shifts at higher pressure when expansion and compression are repeated. This kink could be related to aggregation since molecules start to interact via H – bonds and less energy is required after then to bring them closer. No collapse is observed until  $40 \text{ mN/m}$ . Different pressures were chosen for deposition ( $5 \text{ mN/m}$ ,  $12 \text{ mN/m}$ ,  $18 \text{ mN/m}$ ) and the monolayer is quite stable at all pressures; one example of film stability is reported in Fig. 3 for  $\pi = 12 \text{ mN/m}$ . The pressure-area curve reproducibility has been checked by several experiments.

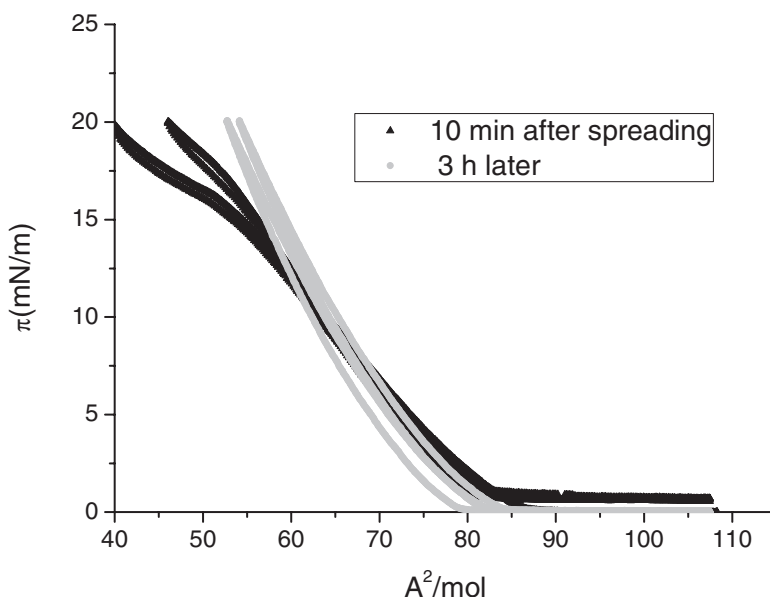


**Figure 2.**  $\pi$ -A curve of [BPY-9ZN(CURC)(Cl)] Langmuir monolayer at air-water interface.

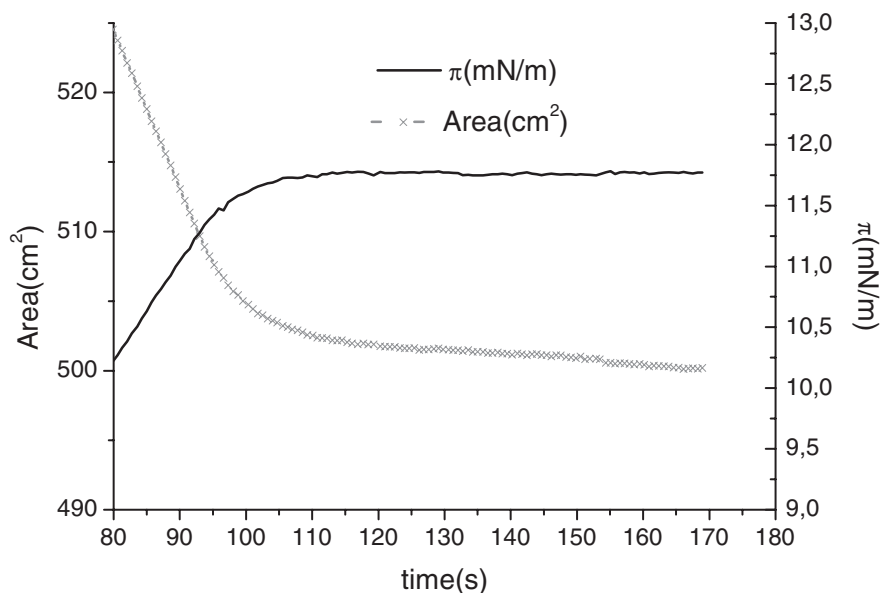


**Figure 3.** Stability of the monolayer at 12 mN/m; the solid curve is the surface pressure while the symbols the surface area.

In Fig. 4a the morphology of LB deposition onto mica for the three different pressures (5, 12, 18 mN/m) is shown: patches of monolayer are clearly observed. The scan area is  $2 \times 2 \text{ micron}^2$ .

As visible from AFM images, by increasing the compressing pressure the film becomes more uniform, i.e. the coverage area increases with the pressure (46%, 73%, 83% respectively) as expected. For the film deposited at 5 mN/m, the monolayer height is about 1.2 nm, 1.3 nm is found for the film deposited at 12 mN/m, and for the last deposition, the height increase slightly up to 1.4 nm. This could be explained considering that the chains gradually raise increasing the surface pressure.

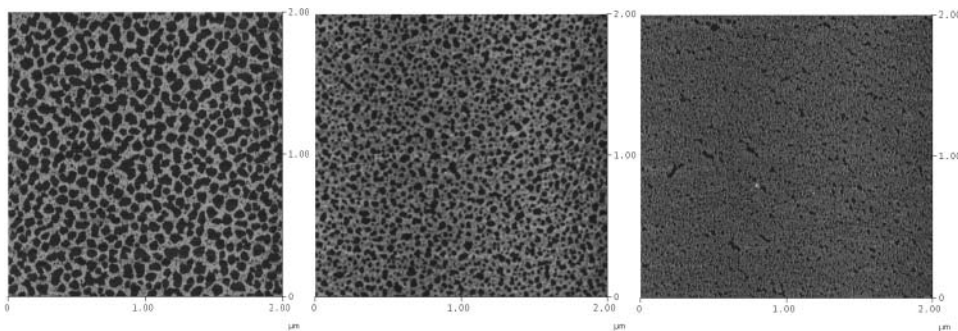


**Figure 4a.** LB monolayer deposition on mica at pressure of 5 mN/m (left), 12 mN/m (centre) and 18 mN/m (right).

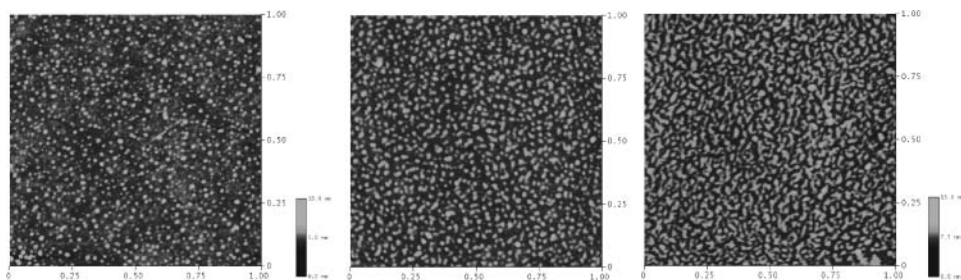


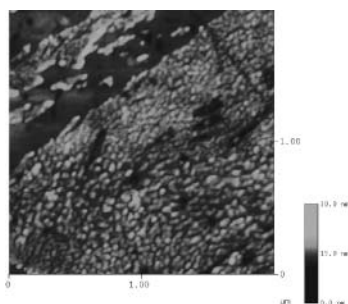
**Figure 4b.** LB monolayer deposition on silicon at pressure of 5 mN/m(left), 12 mN/m(center) and 18 mN/m (right).

The same experiment has been repeated using Langmuir Schaefer deposition on hydrophobic glasses and aggregates are clearly visible on the surface (data not shown); the same morphology is visible on silicon surface: clusters with a height 1.3 nm at 5 mN/m, 2 nm at 12 mN/m and 2.5 nm at 18 mN/m are found. No coverage estimate is done in this case due to the presence of aggregates of different size.

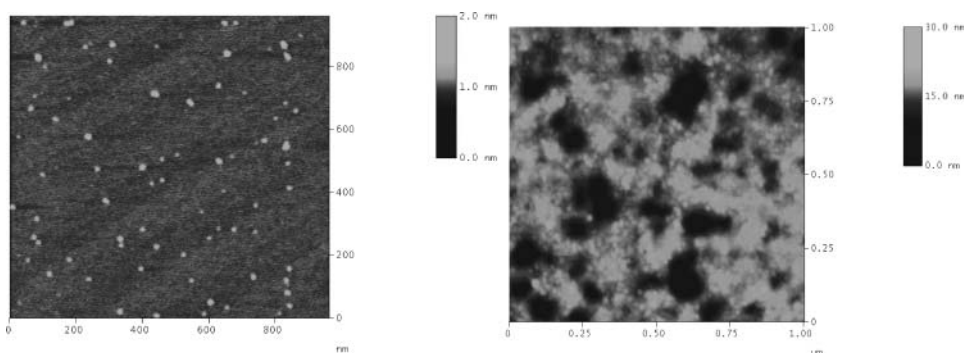
The contact angle for mica is low (less than  $10^\circ$ ) indicating that the surface is very hydrophilic and almost completely wettable as reported in literature [19], while for silicon wafer chemically treated with piranha solution, we found a contact angle of  $30^\circ$ . The surface energy of the two substrates hence is quite different. Usually from  $0$ – $30$  degrees the surfaces are considered as hydrophilic, for tests we deposited the film on silicon wafer either by LS and LB technique. In the first case some water is removed from the surface together with the monolayer, a rearrangement takes place and spherical aggregates form onto the surface (Fig. 4b). In the latter a very rough layer is formed and, due to surface energy difference between mica and silicon, the layer is not transferred into the substrate conserving its morphology like in mica case.

Fig. 4b shows the topography of [BPY-9ZN(CURC)(Cl)] deposited on silicon at pressure of 5, 12, 18 mN/m. At the pressure of 12 and 18 mN/m, it is possible to observe clusters of [BPY-9ZN(CURC)(Cl)] on the surface. The height of this aggregates is about 1.5–2 nm.

Figure 5 shows the topography of [BPY-9ZN(CURC)(Cl)] deposited on glass at pressure of 12 mN/m: also in this case aggregates are visible. The height has been measured considering a section and is about 3 nm, which can consist either with a single straight layer or two molecular layers. From all these measurements it appears clear that deposition on hydrophilic surfaces gives rise to a monolayer quite homogeneous while the deposition



**Figure 5.** LB monolayer deposition on glass at pressure of 12 mN/m scan size  $2 \times 2 \mu\text{m}$ .



**Figure 6.** Spin coating deposition of [BPY-9ZN(CURC)(Cl)] solved in chloroform on mica (left) and glass (right).

on surfaces with lower surface energy gives rise to a not homogeneous layer; this behavior has been confirmed by spin coating measurements described in the following section.

## Spin Coating

The spin coating technique is widely used in liquid crystal research to obtain uniform polymeric layers as alignment layers in liquid crystal cell, hence we decided to use this technique for this molecule.

For all solutions, i.e. [BPY-9ZN(CURC)(Cl)] dissolved in chloroform, ethanol and water, the two depositions on glass and mica are shown together to emphasize the differences in the morphology of the film.

Figure 6 shows the samples obtained from molecule deposition, when dissolved in chloroform, using glass, silicon and mica as substrates. On glass, a very rough film is obtained due to the presence of small aggregates. In this case it is difficult to estimate the film thickness with AFM and the roughness is quite large ( $3.5 \pm 0.1$  nm).

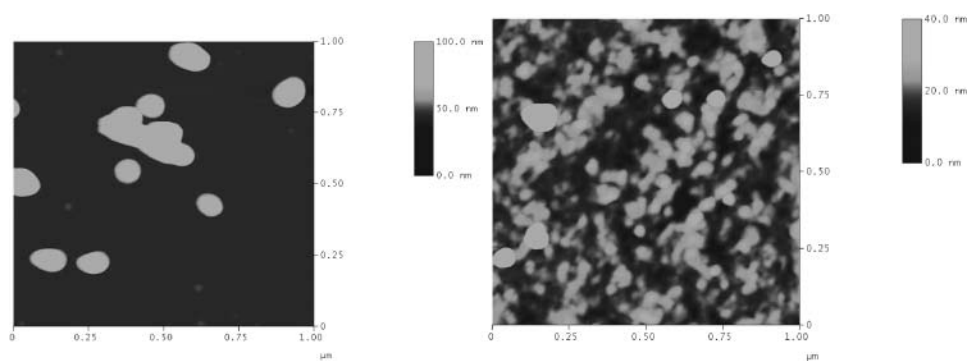
On mica we are able to distinguish small aggregates that could be single molecules, dimers or trimers since from X ray single crystal data it appears that molecules have a volume  $17 \times 2.3 \times 22 \text{ \AA}^3$  [A.Crispini Private communications] and form easily H-bond among them with alternating dipoles. The height of this features on mica ranges from 0,2 nm to 0,6 nm which corresponds to a molecule lying flat on the surface. The tip radius of curvature is about 10 nm, then we can infer that there is a part of the molecular aggregate that it is not accessible for imaging due to the tip shape.

In fact particle analysis gives a distribution of aggregates with a mean diameter of  $16 \pm 4$  nm. The minimum measured diameter is 11 nm. The same morphology is visible spinning water solution on mica.

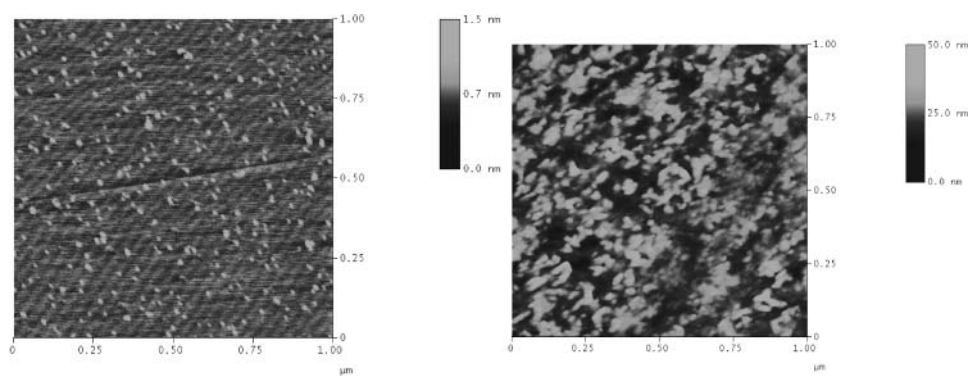
Figure 7 shows the morphology of [BPY-9ZN(CURC)(Cl)] dissolved in ethanol. On mica big aggregates are clearly visible with an height of about 300 nm, instead on glass the film is uniform, characterized by cluster of different size with an average height of 30 nm.

Figure 8 shows the deposition of [Bpy-9Zn(curc)(Cl)] dissolved in water. Similarly to the case of [Bpy-9Zn(curc)(Cl)] dissolved in chloroform, on mica it is possible to distinguish small molecular aggregates, whose height is about 0,5 nm. On glass the covering is quite uniform with a roughness of 5 nm. No film or aggregates are found spin coating water





**Figure 7.** Spin coating deposition of [BPY-9ZN(CURC)(Cl)] solved in ethanol on mica (left) and glass (right).



**Figure 8.** Spin coating deposition of [BPY-9ZN(CURC)(Cl)] solved in water on mica (left) and glass (right).

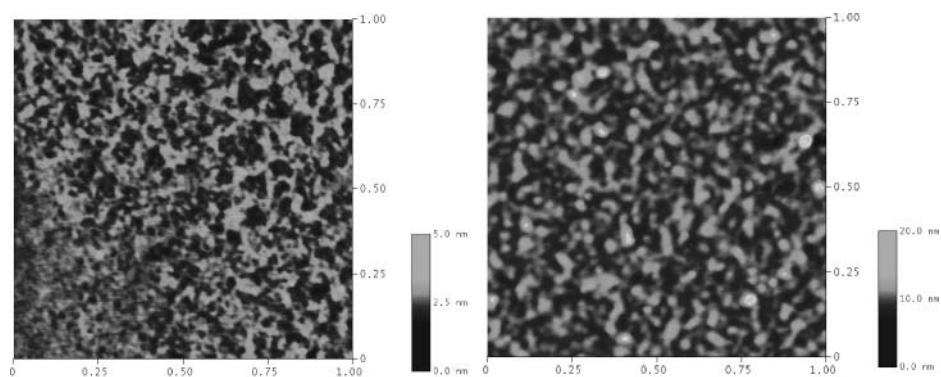


**Figure 9.** Spin coating deposition on silicon from chloroform (left) and ethanol (right) solutions.

solution onto piranha washed silicon. While films, obtained spin coating the other solutions on silicon, present very rough morphology and aggregates of different sizes (Fig. 9).

## Conclusions

The substrate surface energy strongly influences the monolayer deposition.

When [BPY-9ZN(CURC)(Cl)] is deposited by Langmuir Blodgett technique onto mica, it is possible to obtain a uniform coverage of the substrate. By measurements done with AFM we can confirm that is a monomolecular layer with an height of c.a. 1.2 nm, indicating that the long carboxylic chains are slightly tilted. Spin coating depositions were carried out as well to check the film quality obtained with this standard technique. The molecule was in this case dissolved in chloroform, solvent used for LB deposition, ethanol and water. The last two solvents are biocompatible.

As previously shown in the AFM section, using chloroform and water it is possible to observe small molecular aggregates, and to measure their height in order to compare the results with those obtained from single crystal diffraction. The data about height obtained by AFM measurements are in agreement with X ray single crystal data considering that the long chains are not perpendicular to the substrate but are slightly tilted. A deconvolution data analysis is in progress as well as a research for more accurate experimental techniques in order to obtain more information on the lateral dimension of these aggregates as well as on the single molecule shape.

When the solution of [BPY-9ZN(CURC)(Cl)] and ethanol is deposited by spin coating, large aggregates are clearly visible with an average height of 300 nm, even if the molecular solubility is higher in ethanol with respect to other solvents.

Aggregates are also observed when Langmuir Schaefer or spin coating deposition is used either on silicon or on hydrophobic glasses; it is likely that an aggregation process occurs at this interface therein films appear not homogeneous. The influence of this feature, i.e. layer homogeneity, on chromonic molecules alignment is under study. The morphology on hydrophobic HF (hydrofluoric acid) etched silicon surface could be interesting as well even if this kind of substrate is not interesting for future works.

The imaging of anti-cancer new complex on mica is good and preliminary results of its intercalation in DNA phase seem promising as we will show in a further work.

## Acknowledgments

The financial support by MIUR (PRIN2008) "Self-assembly of nucleic acids: a molecular toolbox for soft matter science" is gratefully acknowledged. The authors wish to acknowledge prof. Alessandra Crispini for the fruitful scientific discussions.

## References

- [1] Pucci, D., Crispini, A., Ghedini, M., Pirillo, S., & Liguori, P. F. Complessi di zinco con curcuminoidi come agenti antitumorali. Depositario: Daniela Pucci. Italia C07H015000, Patent no. CS2011A000029 2011.
- [2] Pucci, D., Crispini, A., D'Agnano, I., Liguori, P. F., Garcia-Orduña, P., Pirillo, S., Valentini, A., Bellini, T., & Zanchetta, G. accepted *Chem. Med. Com.*
- [3] Otto, I., & Gust, R. (2007). *Arch. Pharm. Chem. Life Sci.*, 340, 117–126.
- [4] Bruijninx, P. C. A., & Sadler, P. J. (2008). *Curr. Opin. Chem. Biol.*, 12, 197–206.

- [5] Liguori, P. F., Valentini, A., Palma, M., Bellusci, A., Bernardini, S., Ghedini, M., Panno, M. L., Pettinari, C., Marchetti, F., Crispini, A., & Pucci, D. (2010). *Dalton Transactions*, 39(17), 4205–4212.
- [6] Simon, K. A., Burton, E. A., Cheng, F., Varghese, N., Falcone, E. R., Wu, L., & Luk, Y. Y. (2010). *Chemistry of Materials*, 22(8), 2434–2441.
- [7] Lydon, J. (2010). *Journal of Material Chemistry*, 20, 10071–10099.
- [8] Nazarenko, V. G., Boiko, O. P., Park, H.-S., Brodyn, O. M., Omelchenko, M. M., Tortora, L., Nastishin, Yu. A., & Lavrentovich, O. D. (2010). *Phys. Rev. Lett.*, 105(1), 017801.
- [9] Berge, T., Jenkins, N. S., Hopkirk, R. B., Waring, M. J., Edwardson, J. M., & Henderson, R. M. (2002). *Nucleic Acid Research*, 30(13), 2980–2986.
- [10] Berge, T., Haken, E. L., Waring, M. J., & Henderson, R. M. (2003). *Journal of Structural Biology*, 142, 241–246.
- [11] Aleksandra Mihailovic, Ioana Vladescu, Micah McCauley, Elaine Ly, Mark C. Williams. Eileen M. Spain, & Megan E. Nuñez. (2006). *Langmuir*, 22, 4699–4709.
- [12] Coury, J. E., McFail-Isom, L., Presnell, S., Williams, L. D., & Bottomley, L. A. (1995). *J. Vac. Sci. Technol. A*, 13(3), 1746–1751.
- [13] Yi Zhu, Hu Zeng, Jianming Xie, Long Ba, Xiang Gao, & Zuhong Lu. (2004). *Microscopy and Microanalysis*, 10, 286–290.
- [14] Koji Nakano, Yosuke Katsumi, Nobuaki Soh, and Toshihiko Imato. (2010). *Bull. Chem. Soc. Jpn.*, 83(3), 273–275.
- [15] David Pastré, Olivier Piétrement, Alain Zozime, & Eric Le Cam. (2005). *Biopolymers*, 77(1), 53–62.
- [16] Rupert Krautbauera, Lisa H. Popeb, Tobias E. Schradera, Stephanie Allenb, & Hermann E. Gauba. (2002). *FEBS Letters*, 510, 154–158.
- [17] Sampaiolese, B., Bergia, A., Scipioni, A., Zuccheri, G., Savino, M., Samorì, B., & De Santis, P. (October 15, 2002). *PNAS*, 99(21), 13566–13570.
- [18] Roberts, G. (1990). *Langmuir Blodgett Film*, Plenum Press: New York.
- [19] Falini, G., Fermani, S., Conforti, G., & Ripamonti, A. (2002). *Acta Cryst. D*, 58, 1649–16